

# Head Mounted Pupil Tracking Using Convolutional Neural Network

Yinheng Zhu  
Xiamen University

Wanli Chen  
Southern University of Science and Technology

Xun Zhan  
Xiamen University

Zonglin Guo  
University of California, Irvine

Hongjian Shi  
Southern University of Science and Technology

Ian G. Harris  
University of California, Irvine

## ABSTRACT

Pupil tracking is an important branch of object tracking which require high precision. We investigate head mounted pupil tracking which is often more convenient and precise than remote pupil tracking, but also more challenging. When pupil tracking suffers from noise like bad illumination, detection precision dramatically decreases. Due to the appearance of head mounted recording device and public benchmark image datasets, head mounted tracking algorithms have become easier to design and evaluate. In this paper, we propose a robust head mounted pupil detection algorithm which uses a Convolutional Neural Network (CNN) to combine different features of pupil. Here we consider three features of pupil. Firstly, we use three pupil feature-based algorithms to find pupil center independently. Secondly, we use a CNN to evaluate the quality of each result. Finally, we select the best result as output. The experimental results show that our proposed algorithm performs better than the present state-of-art.

## 1 INTRODUCTION

Pupil tracking is a research field in pattern recognition with wide applications. It has been extensively used in gaze estimation [16], game industry [21,22] and psychological analysis [23,24]. The most important indicator for pupil tracking is robustness. A good pupil tracking algorithm should work at many challenging conditions such as low illumination, light reflection and obstacles blocking scenarios with high accuracy. Although pupil tracking is a branch of object tracking, the traditional object tracking algorithms such as CSK [32] and KCF [33] are not suitable in this field because pupil tracking needs higher precision.

There are two approaches for pupil tracking according to the location of sensor. One is remote tracking, which uses a sensor far from tested individuals. These methods are usually combined with face detection and alignment [17], saliency detection [18,19] or using geometric information [20]. The advantage of remote sensing is that it usually has good robustness and less sensitive to noise. However, it needs a fixed camera, which is inconvenient when moving. Another approach for pupil tracking is head mounted sensing. These methods used head mounted device for recording and detection. The main approach for head mounted pupil tracking

is to use low-level characteristics of image such as blob [1-3], edge [4-8] or combining multiple low-level features [9-13]. Head-mounted tracking is more convenient because the tracking device is portable, however, it is usually more sensitive to noise than remote sensing.

Head mounted tracking is essential in rendering VR images [37]. Using pupil tracking to support rendering process will greatly reduce the cost of computation and maintain the visual quality. Therefore, head mounted tracking becomes more and more important.

Previous work in head mounted tracking usually uses CASIA or UBIRIS iris dataset [34-35] or uses a special-purpose dataset. However, almost all pupils in CASIA or UBIRIS datasets are in well illuminated condition, which is not realistic for head mounted tracking and self-recorded dataset may not cover all challenging conditions. In 2014, Pupil Lab released their head mounted tracking device [31], which gives researchers a device for head mounted recording. In 2016, Tonsen M et.al recorded a pupil dataset in wild condition by using Pupil Lab device [27]. The Labeled Pupil in the Wild (LPW) dataset covered people in different races and different challenges in pupil tracking. Due to the appearance of LPW dataset, the evaluation of head mounted tracking becomes feasible.

There are many challenges for head mounted pupil tracking, especially in the wild. The challenges such as bad illumination, eyelashes covering pupil, highly off-axis, reflections, pupil at eye border or image border and border of glasses covering pupil (Fig. 2) make head mounted tracking difficult.

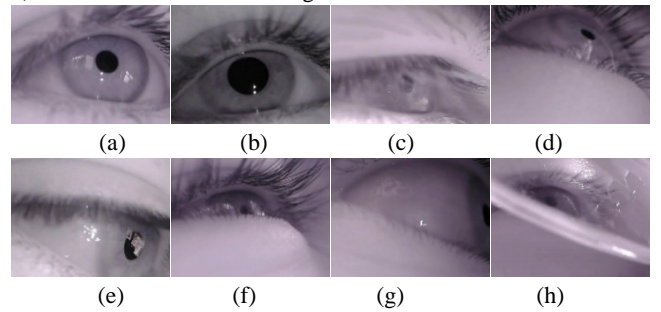


**Figure 2: Challenges in pupil detection. From left to right then up to down is: (a) strong illumination, (b) weak illumination, (c)**

eyelashes covering pupil, (d) highly off-axis, (e) reflections, (f) pupil at eye border or (g) image border and (h) border of glasses covering pupil.

Low-level-characteristics such as edge, color and histogram are often used in pupil detection. However, low-level-characteristic-only methods for pupil tracking have their own limitations that are hard to overcome. For instance, when using histogram characteristic [5] [11], that is, using the two-peak-shape feature in histogram to separate the gray level of eye image, the pupil should in equally illuminated condition and the algorithm will easily break down in unequal illumination (Fig. 3). Edge characteristic detection is now the most commonly used method [4-8], ellipse fitting algorithm [13,14] is usually applied at the end of algorithm to find pupil center. However, these methods are vulnerable, because when there is no clear ellipse-shaped edge, the algorithms will fade. In order to weaken these limitations, high-level-characteristics such as shape and target should be combined in pupil detection. Convolutional Neural Networks show great advantage over other methods in high-level characteristic recognition. Therefore, in this paper, we combine the low-level characteristics with high-level characteristics by using CNN.

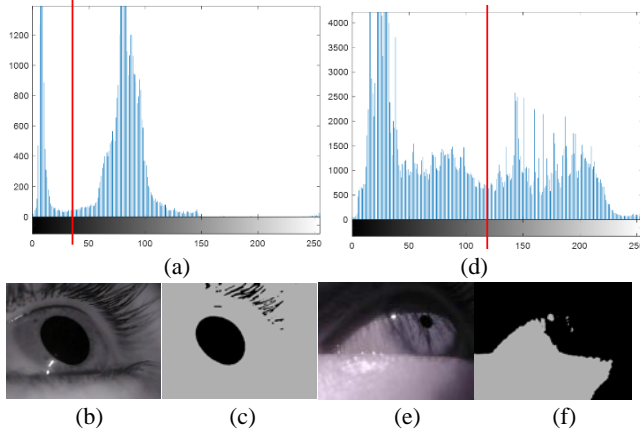


**Figure 3: Limitation of histogram segmentation.** (a) Histogram of pupil in equally illuminated condition. (b) Pupil image in equally illuminated condition. (c) pupil figure of (b) after gray level separation. (d) Histogram of pupil in unequally illuminated condition. (e) Pupil image in unequally illuminated condition. (f) pupil figure of (e) after gray level separation. If eye is illuminated unequally, this method will fade.

Many eye tracking algorithms have appeared in recent years that based on different features. Combining them together can reach a higher robustness. A similar approach for gaze estimation is called “candidate selection” [18]. In paper [18], they identified candidate gaze locations at first. Then they extracted features from the locations. Finally, they estimated the probability of gaze for each candidate according to their features. This idea is applied in our algorithm. In this paper, we focus on blob feature, edge feature and motion feature of pupils. It is obvious that pupil is the darkest area of eyes, which conveys strong blob feature information. Unlike traditional blob detection algorithm used in pupil tracking [1-3] that

only detects dark blobs, our proposed algorithm also calculated the center of light blobs, then uses the center of gravity of dark and light blobs as the pupil center. Edge feature are the most commonly used feature, these methods usually used edge detector to find edge then applied ellipse fitting algorithm to find pupil. The best edge feature detection algorithm ELSe [6] is used in this paper. Motion estimation is also important. When using high-speed camera, pupil shown in two adjacent frames usually has almost the same position. This characteristic can be used to refine the position of detected pupil. In the proposed method, every feature detect algorithm are carried out independently and generating three candidates, then the results will all go through a convolutional neural network [28] to evaluate which one has the best quality and use it as the output. The results show that our proposed algorithm surpasses the current state of art [6] in a third part database by 4.87% in accuracy with 5-pixel error and 6.21% in accuracy with 10-pixel error.

## 2 RELATED WORK

### 2.1 LPW Dataset

Several datasets were created for evaluating the accuracy of different pupil detection methods. The Swirski dataset [5] contains 3760 frames and covers images of both eyes. However, the dataset only provides 600 labelled frames for testing. Therefore, the amount is not sufficient to reach a persuasive result. The ExCuSe dataset [7] includes more frames than Swirski dataset. Later, ExCuSe group improved their algorithm as well as the dataset, adding more frames and covering more illumination conditions. However, to make sure every algorithm will be evaluated fairly, we use a third-part dataset. In this paper, we adopt the LPW dataset [27], which includes high-quality images and using high-speed tracker to record. The dataset also covers different illumination conditions and eyes of people from different ethnicities. The description of LPW dataset [36] is shown in Table. 1.

### 2.2 Convolutional Neural Network Based Algorithms

Convolutional Neural Network (CNN) is a new trend for object tracking as well as pupil tracking. Our approach uses CNN to filter out bad proposals. There are also some previous works using CNN for pupil tracking. Different from our feature selector, they use end-to-end CNN approach to track pupil, such as PupilNet [38] and PupilDeconvNet [39]. The basic framework of them is that they use CNN to find out the region that may contain pupil and select the most possible one as a coarse result at first. Then they apply CNN approach again to find out the fine result on the basis of the coarse result. These end-to-end approaches have great potential.

### 2.3 Swirski, ExCuSe and ELSe Algorithms

**2.3.1 Swirski algorithm.** Swirski [5] algorithm mainly bases on blob feature. It first finds the highest respond to Hair-like feature and then finds the threshold for segmenting the pupil by k-means cluster. After that, RANSAC [14] iteration to find the best ellipse and the center.

**2.3.2 ExCuSe and ELSe algorithm.** ExCuSe [7] and ELSe [6] algorithm both consider the edge feature. ExCuSe algorithm detect

the peak in the gray-scale histogram. If a peak is found, the algorithm applies Canny edge filter and a morphologic method to remove relatively straight lines and thin other curves. The curve that contains the darkest pixels will be selected as the predicted edge. Finally, it uses direct least squares method to fit ellipse and find the center.

ElSe Part I: ElSe, which is similar to ExCuSe, firstly keeps the morphologic method and then uses least squares method to get ellipses. Then the algorithm selects the best one by using a filter (Fig. 4). The width and height of gray, white and black squares are  $1/2$ ,  $1$  and  $2/3$  of the enclosing rectangle of the ellipse. The filter convoluted with the area and if the value exceeds the threshold, then it is the predicted answer.

ElSe Part II: In case there is no ellipse found by the previous method, a second algorithm is adopted. It uses a low pass filter to reduce the influence of noise in the image and then separately convoluted the image with a surface difference filter and a mean filter. The results of the two filters are multiplied and the maximum respond point will be the start point. Afterwards, in the full scaled image, the algorithm selects pixels with gray level under the threshold and use their center of mass as the pupil center. ElSe method is now the state of art and shows better robustness compare with other methods [36].

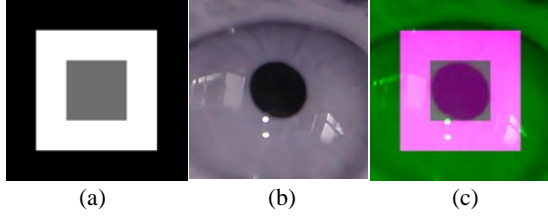


**Figure 4: ElSe ellipse selection filter and its application condition.**

**Table 1: Datasets in LPW**

Dataset	Frames	Description
1	5999	Changing illumination conditions, eyelashes covering pupil
2	6000	Bad illumination
3	6000	Reflections, changing illumination conditions

4	6000	Bad illumination, off-axis, reflections, pupil at border
5	6000	Border of glasses covering pupil, blurred images
6	6000	Eyelashes covering pupil, pupil at border
7	6000	Reflections, small pupil, bad illumination, pupil at border
8	6000	Reflections, small pupil, bad illumination, pupil at border
9	6000	Eyelashes covering pupil, pupil at border
10	6000	Highly off-axis, bad illumination, pupil at border
11	6000	Eyelashes covering pupil, pupil at border
12	6000	Bad illumination, pupil at border
13	5127	Reflections, bad illumination, eyelashes covering pupil
14	6000	Highly off-axis, eyelashes covering pupil
15	6000	Reflections
16	5731	Reflections, bad illumination
17	6000	Highly off-axis, eyelashes covering pupil, bad illumination
18	6000	Reflections, bad illumination
19	6000	Highly off-axis, pupil at border, upside down, reflections
20	6000	Bad illumination, pupil at border
21	6000	Pupil at image border
22	6000	Mascara, pupil at border

### 3 PROPOSED ALGORITHM

The proposed algorithm combines three different features for pupil detection. The tested images are transferred into gray level image at the beginning, then every feature detection algorithm runs independently. After that, the output results are used as input for CNN evaluator to measure which one is the best solution. The three algorithms evaluate pupil position in different aspects. When one approach does not work, the other may work. This complementary characteristic makes the combined algorithm has higher robustness than every candidate algorithm. The whole process is shown in Fig. 1.

#### 3.1 Blob Feature Detection

In blob feature detection, we use simple blob detection algorithm (SBD) with an improvement in detection method. Basic SBD is an algorithm implemented in OpenCV library [25]. The algorithm iteratively extracts connected areas and calculates centers according to certain threshold. To find the center of each area, the algorithm uses different features to limit the edge selection,

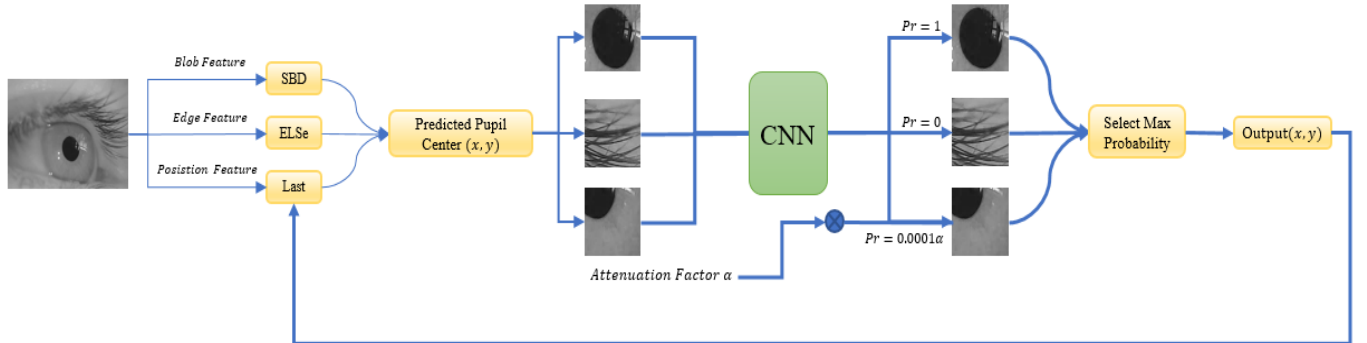


**Figure 1: Process of Proposed Algorithm**

including color, area, circularity, inertia ratio and convexity. The formula for each feature is listed below. Circularity  $C$  is defined as:

$$C = \frac{4\pi S}{\rho^2}$$

$S$  is area of the blob and  $\rho$  is perimeter of the blob. Eccentricity  $E$  is defined as:

$$\begin{aligned} E^2 + I^2 &= 1 \\ \mu_{pq} &= \sum_x \sum_y (x - \bar{x})^p (y - \bar{y})^q f(x, y) \\ \text{cov}[f(x, y)] &= \begin{bmatrix} \mu'_{20} & \mu'_{11} \\ \mu'_{11} & \mu'_{02} \end{bmatrix} = \begin{bmatrix} \mu_{20} & \mu_{11} \\ \mu_{11} & \mu_{02} \end{bmatrix} \\ \lambda_1 &= \frac{\mu'_{20} + \mu'_{02}}{2} + \frac{\sqrt{4\mu_{11}^2 + (\mu'_{20} - \mu'_{02})^2}}{2} \\ \lambda_2 &= \frac{\mu'_{20} + \mu'_{02}}{2} - \frac{\sqrt{4\mu_{11}^2 + (\mu'_{20} - \mu'_{02})^2}}{2} \\ I &= \frac{\lambda_1}{\lambda_2} \end{aligned}$$

$I$  is inertia ratio of the blob area.  $\mu$  is central moment and  $\text{cov}[f(x, y)]$  is covariance matrix. Convexity  $V$  is defined as:

$$V = \frac{S}{H}$$

$S$  is area and  $H$  is convex hull area of the blob. Afterwards, pixels are sorted by distance. Blob radius is calculated as the average of the two pixels in the middle of the queue and its location  $\{\bar{x}, \bar{y}\}$  is calculated as the center of mass as:

$$\begin{aligned} M_{ij} &= \sum_x \sum_y x^i y^j f(x, y) \\ \{\bar{x}, \bar{y}\} &= \left\{ \frac{M_{10}}{M_{00}}, \frac{M_{01}}{M_{00}} \right\} \end{aligned}$$

Next, the algorithm finds new blobs and stores them in new queues while others will be added to current blob queues. Meanwhile, this algorithm also returns the information of the key points. If the number of blobs in a queue is less than a threshold, then it will be excluded from the key point. Otherwise, we use the formula to find the coordinate  $\{x, y\}$  key point.

$$\{x, y\} = \frac{\sum_i q_i \{x_i, y_i\}}{\sum_i q_i}, q_i = I^2$$

Here  $q_i$  is the weight of the blob and  $I$  is the blob inertia ratio.

### 3.2 Our Improvement on SBD

Blob feature based detection has already been implemented in this field [1-3]. However, traditional method may not work when light blobs appear in pupil. We refine the algorithm by not only tracking the dark blob but also using it for track light blob near the dark area. Afterwards, we calculated the center of gravity of the two blobs. Specifically:

$$\begin{cases} X = \frac{\sum_{i=0}^n x_i r_i^2}{\sum_{i=0}^n r_i^2}, \sqrt{(x_0 - x_i)^2 + (y_0 - y_i)^2} < r_0, i \in N^* \\ Y = \frac{\sum_{i=0}^n y_i r_i^2}{\sum_{i=0}^n r_i^2}, \sqrt{(x_0 - x_i)^2 + (y_0 - y_i)^2} < r_0, i \in N^* \end{cases}$$

$$\begin{cases} X = x_0, \sqrt{(x_0 - x_i)^2 + (y_0 - y_i)^2} \geq r_0, i \in N^* \\ Y = y_0, \sqrt{(x_0 - x_i)^2 + (y_0 - y_i)^2} \geq r_0, i \in N^* \end{cases}$$

Here  $(x_0, y_0)$  is the center of dark blob, other  $(x_i, y_i)$  are the center of light blobs and  $r_i$  is the radius of blobs. This process makes SBD algorithm performs better than it is applied only for dark area. The blob selection is shown in Fig. 5. The blue circle represents the dark blob and the green circles represents the light blobs used for center refinement. The red circles represent the abandoned light blobs.

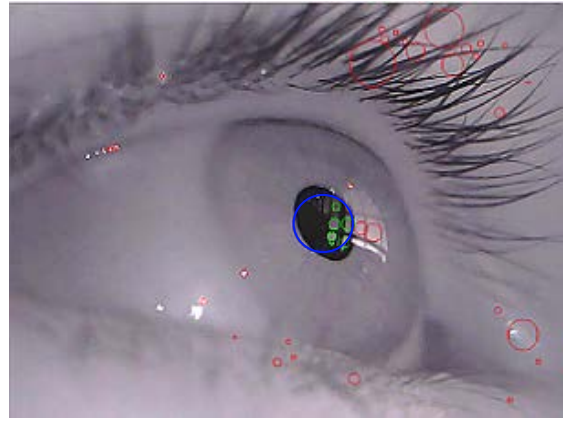


Figure 5: Blob selection in proposed SBD.



Figure 6: Red marker represents pure SBD predicted point, green is enhanced SBD, white is ground truth.

From Fig. 6, we can see that when using basic SBD algorithm (red marker), the detected center will have slight displacement and using the center of gravity of dark blob and light blob (green marker) can “pull” the detected center back to the right place. Although the red marker and green marker almost overlapped in this figure, the red marker is more distant from ground truth with one more pixel error.



Therefore, when dealing with image that has pupil with reflection, our proposed algorithm shows better precision.

The drawback of this algorithm is that when the tested image has unequal illumination, such as Fig. 7(a), the algorithm will not work because the dark area is too big and it is hard to find a center. The proposed algorithm will also lose target when there is no salient dark blob. Then we can conclude that these scenarios do not have obvious blob feature.

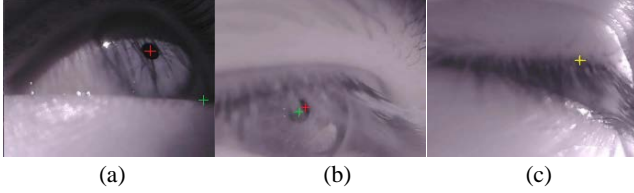


**Figure 7:** In (a) and (b), red marker represents candidate proposed by ELSe, while green marker comes from SBD and white mark is ground truth (cover by red/green marker). In (c), yellow marker represents candidate proposed from motion feature, and white marker is still ground truth (cover by yellow marker).

### 3.3 Edge Feature Detection

In the condition of Fig. 7(a), blob feature is not obvious, however, the edge feature is still salient. Then edge feature detection is applied to deal with this problem. In this part, we only used the part I of ELSe [6], specifically, it applies Canny edge filter to the gray scale image and then refines the edges at first. ELSe provides two different edge filters. The morphologic approach compares several patterns to the edges, which deletes the unnecessary pixels and straightens lines. The algorithm approach is to break up lines and select appropriate ellipses by calculating the changes of angles and distances. As is demonstrated in Fig. 8, if the distance still increases after the angle shrinks from  $90^\circ$  to  $0^\circ$  then a break point will be applied to the divide the edge. Similarly, if the angel increases while the distance increases, the point is considered as a break point.

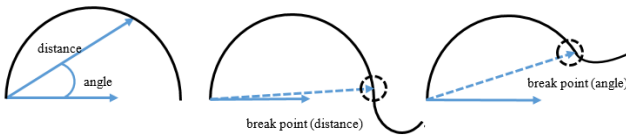


**Figure 8:** ELSe breaking points demonstration.

ELSe implements the morphologic approach as it consumes less computational power. It also provides parameter-adjustable algorithms for both approach. After applying edge filters, the algorithm selects possible ellipses and values each one. The selection of ellipses is based on shape, area and gray value. The score for each ellipse is calculated as

$$\text{eval}(el) = \text{gray}_{\text{value}} * (1 + |el_{\text{width}} - el_{\text{height}}|)$$

$el$  is the ellipse.  $el_{\text{width}}$  and  $el_{\text{height}}$  are semi major axis and semi minor axis.  $\text{gray}_{\text{value}}$  is the inner gray value of the ellipse. It is calculated by applying a pattern based on the ellipse radius. The pattern is demonstrated in Fig. 4.

### 3.4 Substitute of Part II of ELSe

In the proposed algorithm, we only use the part I of ELSe. The reason for not using the latter part is that the part II of ELSe involves many convolution operation, which can slow down the processing speed. Besides, the aim of part II of ELSe is to detect blink and some pupils that covered by many edges. This characteristic is not important in our algorithm, and the reason will be discussed in 3.5.

ELSe algorithm is based on edge feature, which means it also has the innate limitation that other edge-based algorithms have. Fig. 7(b) shows an example. The red marker represents the predicted point generated by ELSe and the green marker is the point generated by SBD, white point represents the ground truth. In this case, eyelashes are covering pupil, which generates many edges and ELSe algorithm has difficulty in recognizing which edge represents pupil while SBD still predicted precisely.

### 3.5 Motion Feature Detection

When applying SBD and ELSe detection, there is a possibility that both of them lose target or detect inaccurately because the pupil is covered (Fig. 7(c)). Therefore, motion estimation is proposed to avoid these scenarios. In this part, we simply let our system remember the position of the last frame. Because in video processing, two adjacent frames are similar. Therefore, when the mentioned scenarios appeared, the pupil position in last frame will be used as the substitute for the pupil position in this frame. The position algorithm can also be used to deal with blink scenarios, which makes it be a good substitute for ELSe part II. Therefore, the ELSe part II is redundant in our algorithm. Actually, the motion feature algorithm always chooses the “last but right” position, that is, if the last position is not accurate, the last position will not be refreshed. The reason is illustrated in 3.6.

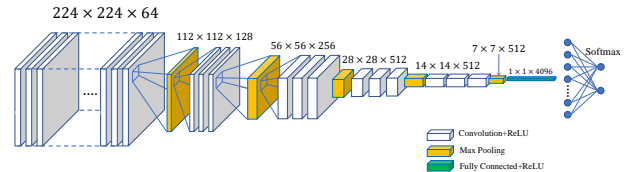


**Figure 9:** CNN decoder using VGG-16.

### 3.6 Position Feature Detection

After finding the predicted points, we used three  $120 \times 120$  pixels' windows that centred in the found points to create three 3-channel sub-images. The chosen window size is  $120 \times 120$  because the whole image size is  $640 \times 480$ . Therefore,  $120 \times 120$  is a relatively large size to guarantee the entire pupil will be covered in the sub-images. When pupil appears at image edge, we pad the sub-image with intensity of 255. The network used in this paper is pre-trained VGG-16. The training images come from different databases [5,6,7,27,34,35]. The positive samples are sub-images that covering pupil and others are negative samples. To avoid overfitting, we only randomly select 8000 frames excluding LPW dataset into our training set. The proportion of positive and negative samples is 1:5 in every batch, batch size is 30. After training, we

input the three sub-images and use the network to score each image and find the one that most similar to pupil. The network is shown in Fig. 9.

Notice that the image between two adjacent frames are similar. Therefore, the motion feature-based algorithm always gets a high score when the last frame is calculated accurately. This effect will make the algorithm bias to motion feature. To avoid this, an attenuation factor  $\alpha(\alpha < 1)$  is applied to scale down the score. After applying that, the motion feature algorithm can only be available when both of SBD and ELSe lose target or detect inaccurately. Also, after applying that, the last frame will only be refreshed on the condition that at least one candidate except last frame gets high score. Therefore, the motion feature algorithm always selects “the last but right” frame. The illustration is shown in Fig. 10.

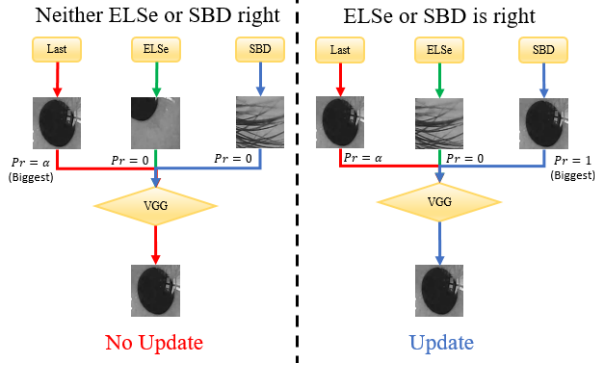


**Figure 10: Scheme of last frame updating.**

The value of attenuation factor is chosen during our experiment. The different curve shows the different accuracy with different attenuation factor. A chart in Fig. 11 shows that After several experiments, we find  $\alpha=0.0005$  shows the best performance in this network. The “motion feature bias” can be easily observed from the chart. When  $\alpha=0.99$ , the accuracy will go down dramatically.

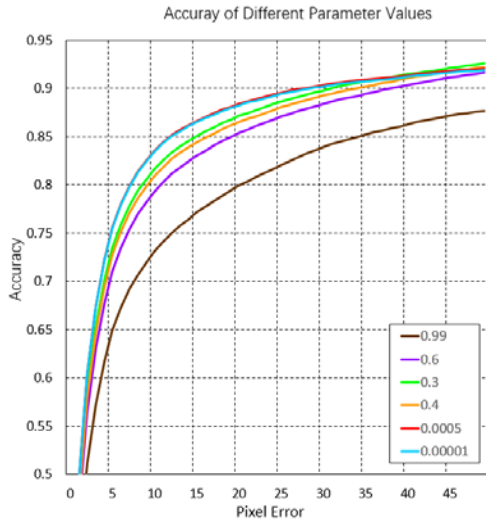


**Figure 11: Experiment on the choice of attenuation factor  $\alpha$ .**

## 4 RESULT AND ANALYSIS

As is previously indicated that ELSe is the current state of art method tested on LPW dataset, according to Fuhl, Wolfgang, et al [36]. Thus, we only compare our algorithm with ELSe. The predicted accuracy will be measured by using the Euclidean distance between ground truth and output result. In paper [36], authors claimed that there is no much difference between ground truth and predicted point if the distance between them is within 5 pixels in 640×480 image. This strict rule is also used in this paper to compare the accuracy of different algorithms. Considering the hand-marked ground truth may not accurate and 5-pixel error may too strict, 10-pixel error is also used to evaluate each algorithm. Beside to the overall performance, some important challenges in VR eye tracking are also tested. Table. 2 shows the speed performance of some algorithms. Our algorithm is under the environment of high performance computer with CPU: Intel(R) Xeon(R) CPU E5-2695 v4 @ 2.10GHz (1 core used), GPU: GeForce GTX 1080.

### 4.1 Overall Performance

The overall performances of different algorithms are evaluated at here. Not only eye tracking algorithms, the traditional object tracking algorithm KCF [33] is also measured in this part.

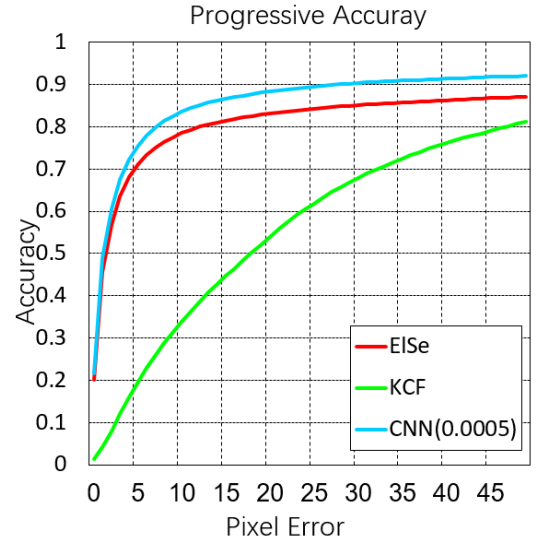


**Figure 12: Overall performance of different algorithms.**

From Fig. 12 we find that our proposed algorithm performs best among all the presented algorithms. Our accuracy in 5-pixel error is 75.53% and 83.51% in 10-pixel error while the accuracy in ELSe is 70.66% and 77.30% in 10-pixel error. Our results surpass the current state of art ELSe by 4.87% in 5-pixel error and 6.21% in 10-pixel error. Besides, the result also shows that traditional object tracking algorithm is not suitable for pupil tracking.

### 4.2 Bad Illumination Condition

One of the challenges in VR eye tracking is that the illumination condition of eyes may change when people watching different

sceneries. Therefore, this condition is measured specifically. LPW dataset provided several bad illumination videos. These videos are used to test different algorithms.

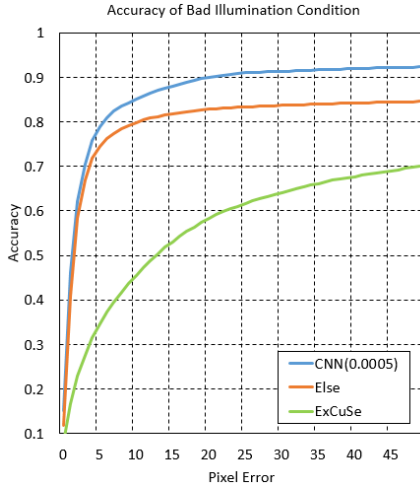


**Figure 13: Accuracy in bad illumination condition.**

The tested datasets in LPW are dataset 3 and 15 because they are recorded in bad illumination condition (Table. 1). From Fig. 13 we find that our proposed algorithm reaches 78.89% accuracy in 5-pixel error while ElSe has 74.52% accuracy. Our proposed algorithm reaches 85.03% accuracy in 10-pixel error while ElSe has 79.8% accuracy. The result shows that our proposed algorithm is more robust in bad illumination conditions.

### 4.3 Reflection Condition

Another important challenge in VR eye tracking is that the light in VR may reflect from eyes. Therefore, this condition is measured specifically. LPW dataset also provided several videos with eye reflection. These datasets are used for testing.

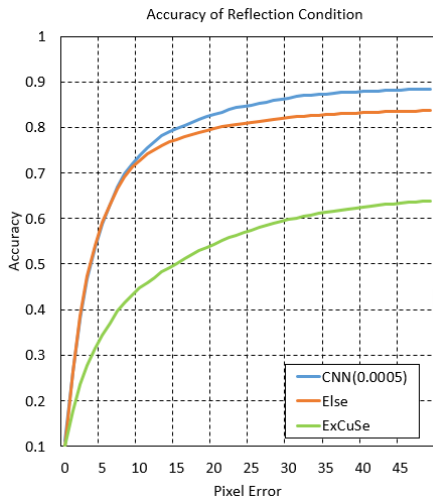


**Figure 14: Accuracy in reflection condition.**

The tested datasets in LPW are dataset 2,4,10,12,20 because they are recorded in reflection condition (Table. 1). From Fig. 14 we find that our proposed algorithm reaches 58.62% accuracy in 5-pixel error while ElSe has 59.09% accuracy. Our proposed algorithm reaches 73.8% accuracy in 10-pixel error while ElSe has 72.76% accuracy. The result shows that our proposed algorithm performs similar as ElSe.

### 4.4 Bad Illumination and Reflection Condition

Bad illumination and reflection can happen at the same time. Then, this scenario is tested.

The tested datasets in LPW are dataset 7,8,13,16,18 because they are recorded in bad illumination and reflection condition (Table. 1). From Fig. 15 we find that our proposed algorithm reaches 81.14% accuracy in 5-pixel error while ELSe has 74.02% accuracy. Our proposed algorithm reaches 88.78% accuracy in 10-pixel error while ELSe has 80.14% accuracy. The result shows that our proposed algorithm is more robust in bad illumination and reflection conditions.

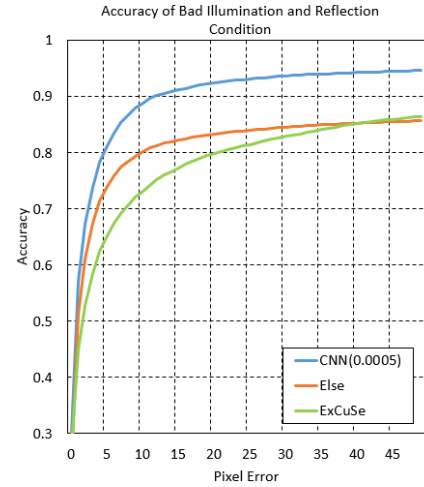


**Figure 15: Accuracy in bad illumination and reflection condition.**

### 4.5 Eyelashes Covering Pupil Condition

Eyelashes may also be disruption in VR eye tracking when users are blinking or get tired. Their eyes model can be simulated by using LPW "eyelashes covering pupil" examples.

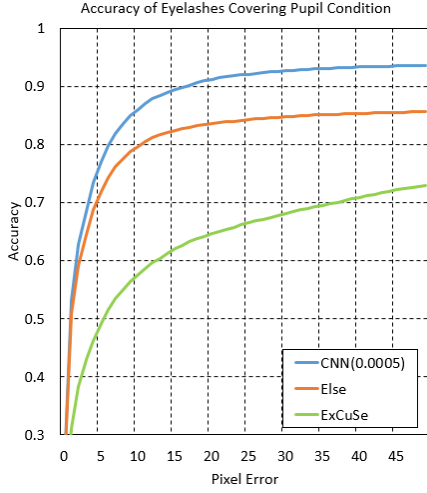


**Figure 16: Accuracy in eyelashes covering pupil condition.**

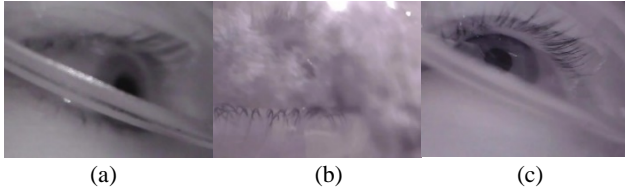
The tested datasets in LPW are dataset 1,6,9,11,13,14,17 because they are recorded in eyelashes covering pupil condition (Table. 1). From Fig. 16 we find that our proposed algorithm reaches 77.09% accuracy in 5-pixel error while ElSe has 71.91% accuracy. Our proposed algorithm reaches 86.01% accuracy in 10-pixel error while ElSe has 79.62% accuracy. The result shows that our proposed algorithm is more robust in eyelashes covering pupil conditions.

## 5 DISCUSSION

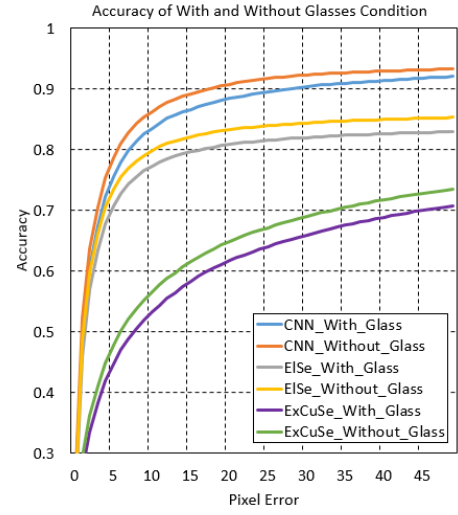
The proposed algorithm performs better than ElSe. However, there are still some problems need to discuss.

### 5.1 Challenging Examples

Some images in LPW dataset are so challenge that even human cannot tell the exact pupil position, especially when people wearing glasses. Because the strong reflection from glasses will make pupil detection rather difficult, the dust on glasses and glass frame are also fatal disruptions for pupil detection, some examples are shown in Fig. 17. These samples are very challenging even to human. To avoid these situations, we can simply place the camera behind glasses. Therefore, we can remove these glasses-worn datasets and re-evaluate our algorithm.



**Figure 17: Some challenging examples. (a) Glass frame covering pupil. (b) Dust on glasses covering pupil. (c) Reflection from glasses.**



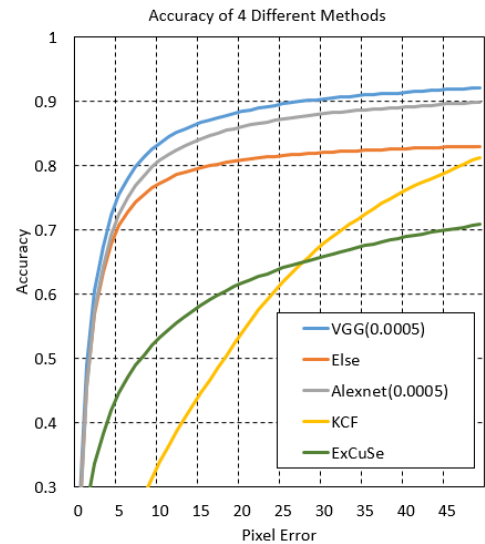
**Figure 18: Accuracy of with/without glasses condition.**

Fig. 18 shows the re-evaluated result. From the picture, we can see that our proposed algorithm still performs better than ElSe. This result is more reasonable in VR pupil tracking condition because some bad samples that cannot happen in VR condition are excluded. The re-evaluated accuracy of proposed algorithm is 78.66% in 5-pixel error and 86.30% in 10-pixel error.

### 5.2 Using AlexNet

Computation speed is vital for VR application. Using VGG net can reach a higher accuracy in the sacrifice of computation speed. AlexNet [29] is shallower than VGG-16. Therefore, it can reach a higher speed. The evaluation of AlexNet is proposed in this part.

The result in Fig. 19. shows that the accuracy of using AlexNet is lower than using VGG-16, but it is still higher than ElSe. Table. 2 shows that the computational speed of using AlexNet is faster than using VGG-16. This result can be used as a trade-off between speed and accuracy.





**Figure 19: Accuracy of 4 different methods.**

**Table 2: Performance of Different Algorithms**

	ExCuSe	ElSe	Proposed (VGG)	Proposed (AlexNet)
Frame Rate	16FPS	25FPS	10FPS	15FPS

## 6 CONCLUSION

In this paper, a multiple feature-based pupil tracking algorithm is proposed. It based on different features that appear in a pupil. The proposed algorithm uses a convolutional neural network to create a judging criterion of different feature based algorithms and choose the best one for tracking. Our algorithm shows a better accuracy among the tested algorithm. The proposed method can be enhanced in speed by using different CNNs.

## REFERENCES

- [1] Choi, Kang-A., et al. "Improved pupil center localization method for eye-gaze tracking-based human-device interaction." Consumer Electronics (ICCE), 2014 IEEE International Conference on. IEEE, 2014.
- [2] Heyman, Tom, Vincent Spruyt, and Alessandro Ledda. "3d face tracking and gaze estimation using a monocular camera." 2nd International Conference on Positioning and Context-Awareness (POCA-2011). 2011.
- [3] Morimoto, Carlos Hitoshi, et al. "Pupil detection and tracking using multiple light sources." Image and vision computing 18.4 (2000): 331-335.
- [4] Kohlbecher, Stefan, et al. "Calibration-free eye tracking by reconstruction of the pupil ellipse in 3D space." Proceedings of the 2008 symposium on Eye tracking research & applications. ACM, 2008.
- [5] Świrski, Lech, Andreas Bulling, and Neil Dodgson. "Robust real-time pupil tracking in highly off-axis images." Proceedings of the Symposium on Eye Tracking Research and Applications. ACM, 2012.
- [6] Fuhl, Wolfgang, et al. "Else: Ellipse selection for robust pupil detection in real-world environments." Proceedings of the Ninth Biennial ACM Symposium on Eye Tracking Research & Applications. ACM, 2016.
- [7] Fuhl, Wolfgang, et al. "Excuse: Robust pupil detection in real-world scenarios." International Conference on Computer Analysis of Images and Patterns. Springer, Cham, 2015.
- [8] Lin, Lin, et al. "A robust and accurate detection of pupil images." Biomedical Engineering and Informatics (BMEI), 2010 3rd International Conference on. Vol. 1. IEEE, 2010.
- [9] Li, Dongheng, David Winfield, and Derrick J. Parkhurst. "Starburst: A hybrid algorithm for video-based eye tracking combining feature-based and model-based approaches." Computer Vision and Pattern Recognition-Workshops, 2005. CVPR Workshops. IEEE Computer Society Conference on. IEEE, 2005.
- [10] Appel, Tobias, Thiago Santini, and Enkelejd Kasneci. "Brightness-and motion-based blink detection for head-mounted eye trackers." Proceedings of the 2016 ACM International Joint Conference on Pervasive and Ubiquitous Computing: Adjunct. ACM, 2016.
- [11] Huang, Junzhou, et al. "A new iris segmentation method for recognition." Pattern Recognition, 2004. ICPR 2004. Proceedings of the 17th International Conference on. Vol. 3. IEEE, 2004.
- [12] Koh, Jaehan, Venu Govindaraju, and Vipin Chaudhary. "A robust iris localization method using an active contour model and hough transform." Pattern Recognition (ICPR), 2010 20th International Conference on. IEEE, 2010.
- [13] Lai, Chih-Chuan, Sheng-Wen Shih, and Yi-Ping Hung. "Hybrid method for 3-D gaze tracking using glint and contour features." IEEE Transactions on Circuits and Systems for Video Technology 25.1 (2015): 24-37.
- [14] Fischler, Martin A., and Robert C. Bolles. "Random sample consensus: a paradigm for model fitting with applications to image analysis and automated cartography." Communications of the ACM 24.6 (1981): 381-395.
- [15] Fitzgibbon, Andrew, Maurizio Pilu, and Robert B. Fisher. "Direct least square fitting of ellipses." IEEE Transactions on pattern analysis and machine intelligence 21.5 (1999): 476-480.
- [16] Hansen, Dan Witzner, and Qiang Ji. "In the eye of the beholder: A survey of models for eyes and gaze." IEEE transactions on pattern analysis and machine intelligence 32.3 (2010): 478-500.
- [17] Zhang, Xucong, et al. "Appearance-based gaze estimation in the wild." Proceedings of the IEEE Conference on Computer Vision and Pattern Recognition. 2015.
- [18] Rudoy, Dmitry, et al. "Learning video saliency from human gaze using candidate selection." Proceedings of the IEEE Conference on Computer Vision and Pattern Recognition. 2013.
- [19] Sugano, Yusuke, Yasuyuki Matsushita, and Yoichi Sato. "Appearance-based gaze estimation using visual saliency." IEEE transactions on pattern analysis and machine intelligence 35.2 (2013): 329-341.
- [20] Cheung, Yiu-ming, and Qinnmu Peng. "Eye gaze tracking with a web camera in a desktop environment." IEEE Transactions on Human-Machine Systems 45.4 (2015): 419-430.
- [21] Corcoran, Peter M., et al. "Real-time eye gaze tracking for gaming design and consumer electronics systems." IEEE Transactions on Consumer Electronics 58.2 (2012).
- [22] Smith, J. David, and T. C. Graham. "Use of eye movements for video game control." Proceedings of the 2006 ACM SIGCHI international conference on Advances in computer entertainment technology. ACM, 2006.
- [23] Johansson, Gunnar. "Visual perception of biological motion and a model for its analysis." Perception & psychophysics 14.2 (1973): 201-211.
- [24] Mele, Maria Laura, and Stefano Federici. "Gaze and eye-tracking solutions for psychological research." Cognitive processing 13.1 (2012): 261-265.
- [25] [http://docs.opencv.org/2.4/modules/features2d/doc/common\\_interfaces\\_of\\_feature\\_detectors.html?highlight=simpleblobdetector#SimpleBlobDetector:public FeatureDetector](http://docs.opencv.org/2.4/modules/features2d/doc/common_interfaces_of_feature_detectors.html?highlight=simpleblobdetector#SimpleBlobDetector:public FeatureDetector)
- [26] Suzuki, S. and Abe, K., Topological Structural Analysis of Digitized Binary Images by Border Following. CVGIP 30 1, pp 32-46 (1985)
- [27] Tonsen, Marc, et al. "Labelled pupils in the wild: a dataset for studying pupil detection in unconstrained environments." Proceedings of the Ninth Biennial ACM Symposium on Eye Tracking Research & Applications. ACM, 2016.
- [28] Simonyan, Karen, and Andrew Zisserman. "Very deep convolutional networks for large-scale image recognition." arXiv preprint arXiv:1409.1556 (2014).
- [29] Krizhevsky, Alex, Ilya Sutskever, and Geoffrey E. Hinton. "Imagenet classification with deep convolutional neural networks." Advances in neural information processing systems. 2012.
- [30] Szegedy, Christian, et al. "Going deeper with convolutions." Proceedings of the IEEE conference on computer vision and pattern recognition. 2015.
- [31] Kassner, Moritz, William Patera, and Andreas Bulling. "Pupil: an open source platform for pervasive eye tracking and mobile gaze-based interaction." Proceedings of the 2014 ACM international joint conference on pervasive and ubiquitous computing: Adjunct publication. ACM, 2014.
- [32] Henriques, João F., et al. "Exploiting the circulant structure of tracking-by-detection with kernels." European conference on computer vision. Springer, Berlin, Heidelberg, 2012.
- [33] Henriques, João F., et al. "High-speed tracking with kernelized correlation filters." IEEE Transactions on Pattern Analysis and Machine Intelligence 37.3 (2015): 583-596.
- [34] Set, Iris Data. "Comments on the CASIA version 1.0 iris data set." IEEE Transactions on Pattern Analysis and Machine Intelligence 29.10 (2007):1.
- [35] Proença, Hugo, and Luís A. Alexandre. "UBIRIS: A noisy iris image database." International Conference on Image Analysis and Processing. Springer, Berlin, Heidelberg, 2005.
- [36] Fuhl, Wolfgang, et al. "Pupil detection for head-mounted eye tracking in the wild: an evaluation of the state of the art." Machine Vision and Applications 27.8 (2016): 1275-1288.
- [37] Pai, Yun Suen, et al. "GazeSim: simulating foveated rendering using depth in eye gaze for VR." ACM SIGGRAPH 2016 Posters. ACM, 2016.
- [38] Fuhl, Wolfgang, et al. "PupilNet: Convolutional Neural Networks for Robust Pupil Detection." Revista De Odontologia Da Unesp 19.1(2016):806-821.
- [39] Vera-Olmos, F. J., and N. Malpica. "Deconvolutional Neural Network for Pupil Detection in Real-World Environments." International Work-Conference on the Interplay Between Natural and Artificial Computation Springer, Cham, 2017:223-231.